Fusion Engineering and Design 124 (2017) 437–441

Contents lists available at ScienceDirect

Fusion Engineering and Design

journal homepage: www.elsevier.com/locate/fusengdes

Analysis of steady state thermal-hydraulic behaviour of the DEMO divertor cassette body cooling circuit

P.A. Di Maio[a], S. Garitta[a], J.H. You[b], G. Mazzone[c], E. Vallone[a,*]

[a] University of Palermo, Viale delle Scienze, Edificio 6, 90128 Palermo, Italy
[b] Max Planck Institute of Plasma Physics (E2 M), Boltzmann Str.2, 85748 Garching, Germany
[c] Department of Fusion and Technology for Nuclear Safety and Security, ENEA C.R. Frascati, via E. Fermi 45, 00044 Frascati, Roma, Italy

HIGHLIGHTS

- Thermal-hydraulic study of DEMO divertor cassette body cooling system.
- Adoption of a computational fluid-dynamic approach based on finite volume method.
- Comparative study on both water and helium cooling options.
- Assessment of spatial distributions of pressure drop, flow velocity and temperature.
- Analysis of an improved layout, leading to significant performances enhancement.

ARTICLE INFO

Article history:
Received 3 October 2016
Received in revised form 26 January 2017
Accepted 5 February 2017
Available online 8 February 2017

Keywords:
DEMO
Divertor
Cassette body
CFD analysis
Thermofluid-dynamics

ABSTRACT

Within the framework of the Work Package DIV 1 – "Divertor Cassette Design and Integration" of the EUROfusion action, a research campaign has been jointly carried out by ENEA and University of Palermo to investigate the thermal-hydraulic performances of the DEMO divertor cassette cooling system. A comparative evaluation study has been performed considering the two different options under consideration for the divertor cassette body coolant, namely subcooled pressurized water and helium.

The research activity has been carried out following a theoretical-computational approach based on the finite volume method and adopting a qualified Computational Fluid-Dynamic (CFD) code.

CFD analyses have been carried out for the considered options of cassette body cooling circuit under nominal steady state conditions and the pertaining thermal-hydraulic performances have been assessed in terms of overall coolant thermal rise, coolant total pressure drop, flow velocity and pumping power, to check whether they comply with the corresponding limits. Results obtained are reported and critically discussed.

1. Introduction

The recent European Fusion Development Agreement roadmap was elaborated to pursue fusion as a sustainable, secure and commercial energy source [1]. In this framework, the divertor is a fundamental component of fusion power plants, being primarily responsible for power exhaust and impurity removal via guided plasma exhaust. Due to its position and functions, the divertor has to sustain very high heat and particle fluxes arising from the plasma (up to 20 MW/m^2), while experiencing an intense nuclear deposited power, which could jeopardize its structure and limit its lifetime. Therefore, attention has to be paid to the thermal-hydraulic design of its cooling system, in order to ensure a uniform and proper cooling, without an unduly high pressure drop.

Within the framework of the activities foreseen by the WP-DIV 1 "Divertor Cassette Design and Integration" of the EUROfusion action, a research campaign has been carried out at the University of Palermo, in cooperation with ENEA, to investigate the steady state thermal-hydraulic performances of the DEMO divertor cassette body cooling circuit, paying a specific attention to the two different options under consideration for its coolant, namely subcooled pressurized water and helium.

The research campaign has been carried out following a theoretical-numerical approach based on the Finite Volume Method and adopting the commercial Computational Fluid-Dynamic (CFD) code ANSYS CFX v.16.2, typically employed also

* Corresponding author.
E-mail address: eugenio.vallone@unipa.it (E. Vallone).

http://dx.doi.org/10.1016/j.fusengdes.2017.02.012
0920-3796/

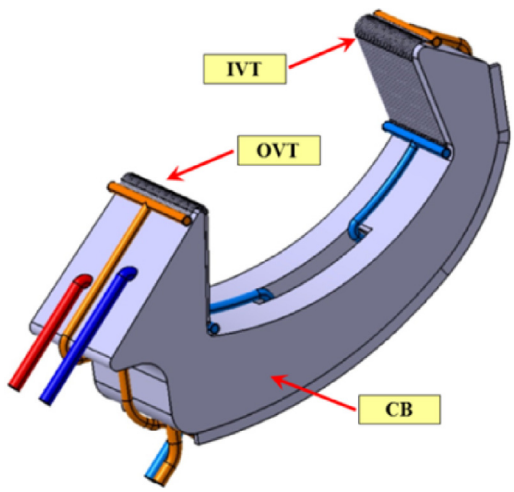

Fig. 1. DEMO divertor cassette 2015 design.

Table 1
Summary of CB cooling options.

	WCDC1	WCDC2	HCDC	HCDC+B4C
Power [MW]	96	96	47	56
Power/cassette [MW]	1.778	1.778	0.870	1.037
Inlet pressure [MPa]	3.5	15.5	4.0	4.0
T_{in} [°C]	150	285	350	350
T_{out} [°C]	220	325	500	500
ΔT [°C]	70	40	150	150
<c_p> [J/kg °C]	4451	5782	5195	5195
G [kg/s]	5.71	7.69	1.12	1.33

to evaluate concentrated hydraulic resistances to be used in system codes [2,3]. The analysis models and assumptions are herein reported and critically discussed, together with the main results obtained.

2. Cassette body cooling circuit

According to its 2015 design, DEMO divertor is composed of 54 toroidal cassettes, each articulated in a Cassette Body (CB) that supports two target plate plasma facing components, namely an Inner Vertical Target (IVT) and an Outer Vertical Target (OVT) (Fig. 1) [4,5].

Four different cooling options are currently under consideration for the CB cooling circuit, that differ both as to coolant, namely pressurized water for Water Cooled Divertor Cassette (WCDC) options and helium for Helium Cooled Divertor Cassette (HCDC) options [6], and to their operative parameters. A summary of the main CB cooling options has been reported in Table 1, together with a preliminary assessment of their thermal-hydraulic performances, carried out assuming nuclear heating data drawn from [7].

Table 3
Summary of assumptions, models and BCs.

	HCDC + B4C	WCDC1
Material library	He ideal gas	IAPWS IF97
Turbulence model	k-ε	k-ε
Boundary layer	Wall functions	Wall functions
Wall roughness	15 μm	15 μm
Nuclear heating [MWm^{-3}]	Data from [7]	Data from [7]
Inlet BC	T_{in} = 350 °C p_s = 4.0 MPa	T_{in} = 150 °C p_s = 3.5 MPa
Outlet BC	G = 1.33 kg/s	G = 5.71 kg/s

3. CB cooling circuit CFD analysis

The thermal-hydraulic performances of both the HCDC + B4C and WCDC1 cooling options currently under consideration for the CB cooling circuit have been investigated under nominal conditions by running separate, steady state, fully-coupled fluid-structure CFD analyses with the ANSYS CFX v.16.2 code.

In particular, CFD analyses have aimed to assess the CB thermal-hydraulic performances in terms of:

- coolant flow velocity distribution;
- coolant overall pressure drop;
- coolant temperature distribution;
- CB structure temperature distribution.

Moreover, for each cooling option two CB design concepts have been studied, namely Design Concept I (DC-I), representing the initial CB reference layout, and Design Concept II (DC-II), differing in flow paths and internal rib thickness from the previous and set-up to overcome the critical issues revealed by CFD analysis.

Selected mesh parameters and main assumptions, models and boundary conditions (BCs) adopted, matured as a further development of [8], are summarized in Tables 2 and 3. A detail of the typical mesh set-up is shown in Fig. 2.

3.1. DC-I CFD analysis results

The fluid and structure calculation domain adopted for the DC-I CFD analysis is reported in Fig. 3.

Steady state CFD analyses have been carried out for both the HCDC + B4C and WCDC1 options to assess their cooling effectiveness by checking whether they allow the structure thermal field to stay below the maximum allowable EUROFER temperature of 550 °C [9] while avoiding the occurrence of coolant saturation, even locally at the fluid-wall interface.

As to the HCDC + B4C cooling option, coolant flow velocity and CB structure temperature distributions are reported in Figs. 4 and 5, showing some issues mainly concerning the structure tempera-

Table 2
Summary of the selected mesh parameters.

Region	Mesh Parameter		DC-I	DC-II
Fluid	**Nodes**		$8.06 \cdot 10^{+6}$	$9.42 \cdot 10^{+6}$
	Elements		$2.02 \cdot 10^{+7}$	$2.38 \cdot 10^{+7}$
	Inflation layers number		12	12
	First layer thickness [μm]		200	200
	Layers growth rate		1.4	1.4
	Typical element size [m]		$6.48 \cdot 10^{-3}$	$9.04 \cdot 10^{-3}$
	Average y^+	**HCDC + B4C**	26.9	21.6
		WCDC1	14.1	15.1
	Min/Max y^+	**HCDC + B4C**	0.01/322	0.03/294
		WCDC1	0.04/201	0.02/149
Structure	**Nodes**		$4.79 \cdot 10^{+6}$	$4.73 \cdot 10^{+6}$
	Elements		$2.39 \cdot 10^{+7}$	$2.39 \cdot 10^{+7}$

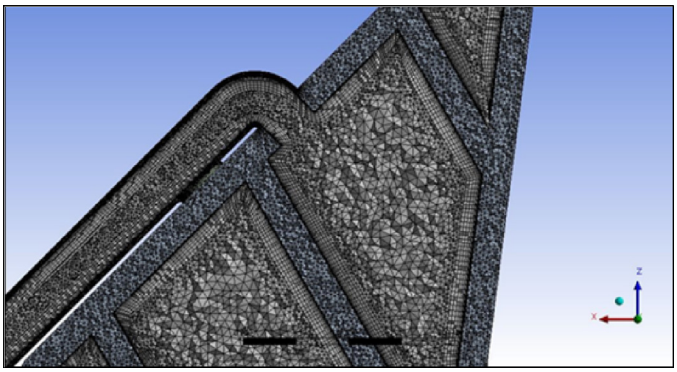

Fig. 2. Detail of a typical mesh set-up.

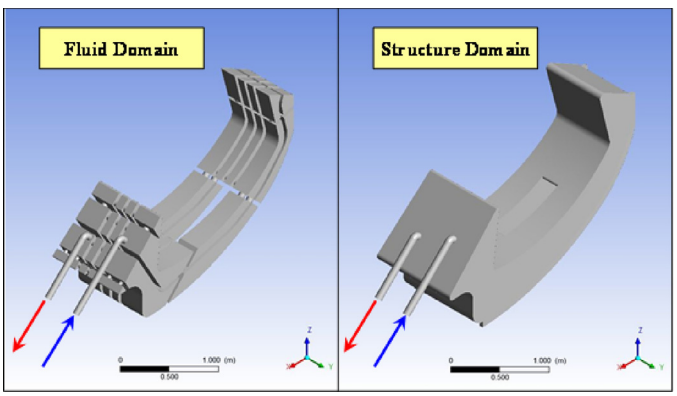

Fig. 3. DC-I fluid and structure calculation domain.

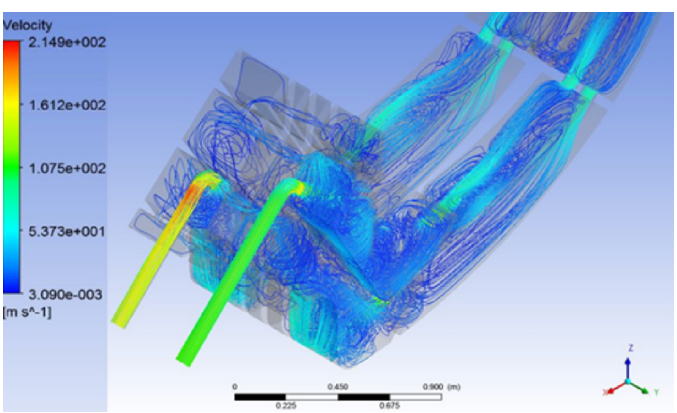

Fig. 4. DC-I: HCDC + B4C coolant flow velocity field.

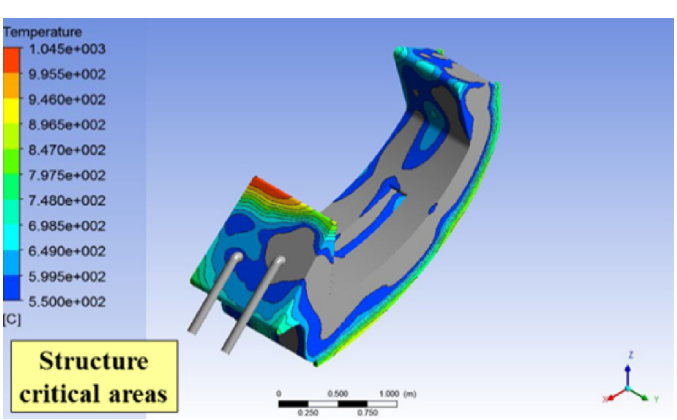

Fig. 5. DC-I: HCDC + B4C structure temperature field.

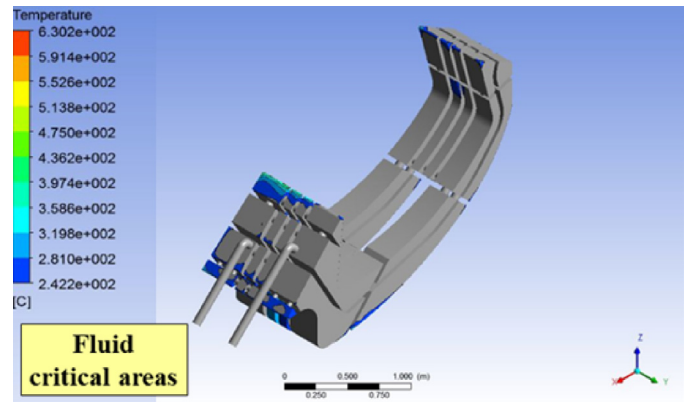

Fig. 6. DC-I: WCDC1 coolant temperature field.

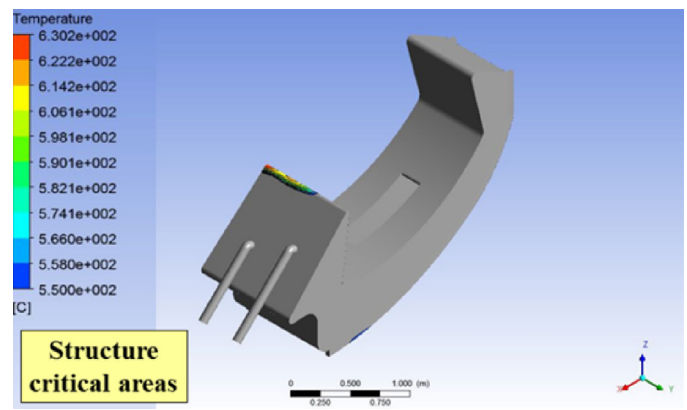

Fig. 7. DC-I: WCDC1 structure temperature field.

Table 4
DC-I CFD analyses main results.

	HCDC + B4C	WCDC1
Δp [MPa]	0.1809	0.0096
Pumping power [kW]	78.547	0.058
ΔT [°C]	153.6	70.9
Fluid T_{max} [°C]	704.2	293.3
Structure T_{max} [°C]	1045.4	630.2

ture field. In fact, Fig. 5 shows wide critical areas where the wall temperature overcomes the limit of 550 °C.

As to the WCDC1 cooling option, coolant and CB structure temperature distributions are reported in Figs. 6 and 7, indicating the occurrence of CB critical areas.

In particular, Fig. 6 shows the coolant critical areas, conservatively defined as the regions where water temperature overcomes the saturation temperature at the minimum pressure reached inside the flow domain. Fig. 7 shows localized critical areas where the wall temperature exceeds the limit of 550 °C. Finally, Table 4 summarizes the main results obtained for both cooling options CFD analyses, additionally showing that there are more than three orders of magnitude between helium and water coolant calculated pumping power.

3.2. DC-II CFD analysis results

In order to improve the thermal-hydraulic performances of DC-I, and particularly those relevant to the structure thermal field, the CB DC-II has been purposely devised. Specifically, the position of inlet/outlet manifolds attachment has been changed (Fig. 8) and the thickness of the structure and of its internal ribs has been decreased

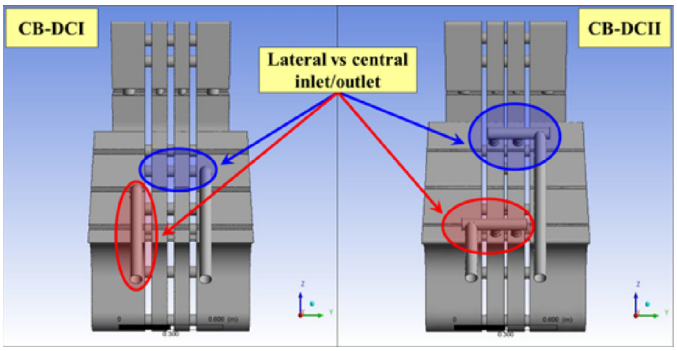

Fig. 8. DC-I and DC-II manifolds attachment.

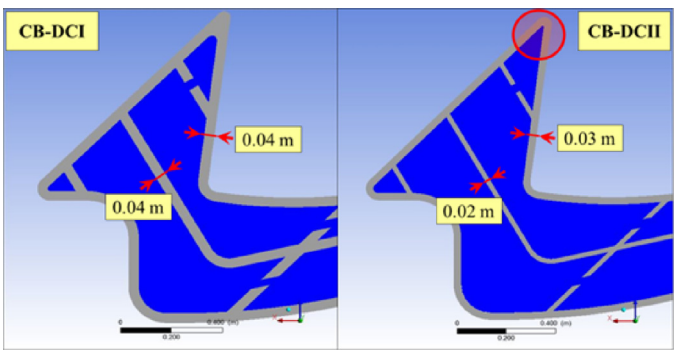

Fig. 9. DC-I and DC-II structural differences.

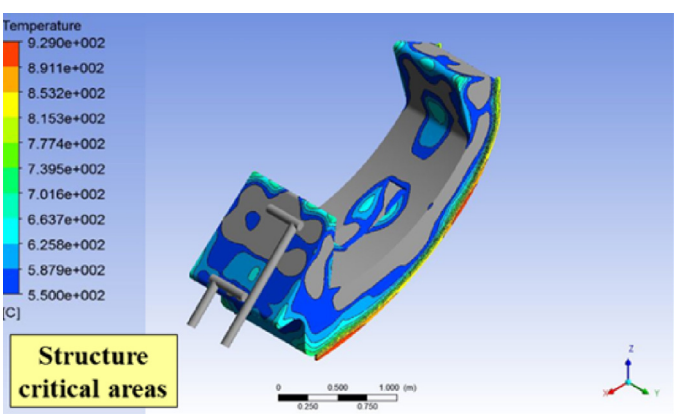

Fig. 10. DC-II: HCDC + B4C structure temperature field.

by a factor 1.3 ÷ 2 along with that of the corners under IVT and OVT (Fig. 9). These changes have aimed to improve flow uniformity and, in general, to enhance the cassette cooling effectiveness.

In analogy with the previous cases, steady state CFD analyses have been carried out for the HCDC + B4C and the WCDC1 cooling options.

Results obtained have shown that, as it was forecast, temperature fields globally assess at lower values. EUROFER maximum temperature (550 °C) is overcome in large areas of CB structure only for HCDC + B4C (Fig. 10). Furthermore, only extremely localized coolant vaporization is predicted as to WCDC1 (Fig. 11). Finally, Table 5 summarizes the main results obtained, additionally showing a limited increase in the evaluated pressure drops and pumping power.

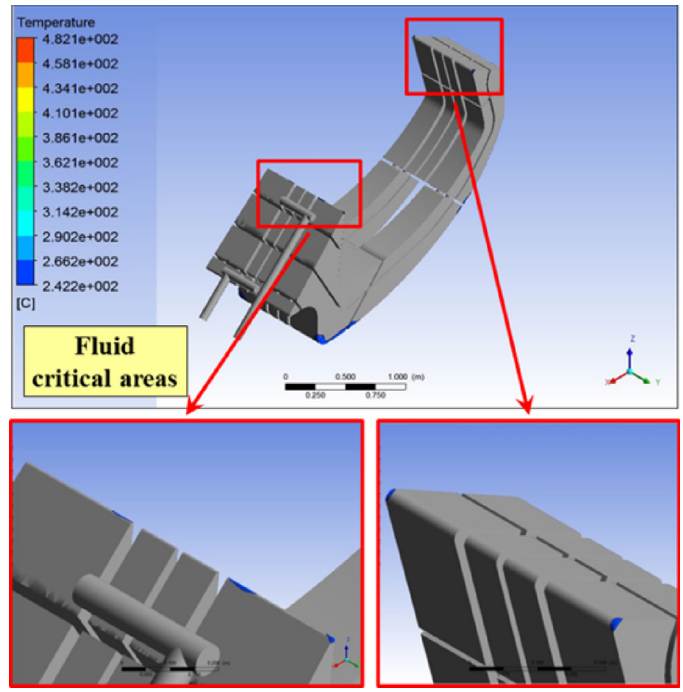

Fig. 11. DC-II: WCDC1 coolant temperature field.

Table 5
DC-II CFD analyses main results.

	HCDC + B4C	WCDC1
Δp [MPa]	0.2108	0.0122
Pumping power [kW]	92.068	0.076
ΔT [°C]	149.1	70.3
Fluid T_{max} [°C]	610.2	242.4
Structure T_{max} [°C]	929.0	482.1

4. Conclusions

Within the framework of the activities foreseen in the WPDIV of the EUROfusion Consortium, a computational study has been carried out at the University of Palermo, in cooperation with ENEA, to investigate the steady state thermal-hydraulic cooling performances of the divertor CB cooling circuit. In order to accomplish this task, two different design concepts have been investigated, namely DC-I and DC-II. For both cases, a helium-cooled (HCDC + B4C) and a water-cooled (WCDC1) option was considered, respectively.

The study has represented the first step of the CB conceptual design and it has been uniquely intended to have a preliminary assessment of the thermal-hydraulic performances of the two cooling options under consideration, starting from a "first-attempt" design of the circuit, as a common basis for both the two cooling options, to be further revised according to the CFD analysis indications so to improve the performances of each cooling option.

Results obtained for the DC-I case indicated that the layout needs to be revised, since its behaviour does not fully meet the requirements of safety and operation temperature limits. In particular, structural material always exceeds the maximum allowed temperature (550 °C), no matter what the adopted coolant was. Moreover, water coolant is expected to experience vaporizations extensively. The flow path also needs to be improved in order to reach more effective cooling, particularly at the outboard CB corners. As for DC-II option, the structure and the flow paths were revised. As a consequence, the temperature level of the structural material could be largely reduced while the maximum allowed temperature was violated only in the case of helium cooling. In

addition, water cooling does not lead to significant vaporization. Finally, pressure drops predicted for this concept are slightly higher than those of DC-I, regardless of coolant. As for the required pumping power for all 54 Cassettes, it ranged between 4.24 MW and 4.97 MW for helium cooling and between 3 and 4 kW in the case of water cooling.

In conclusion, the CB thermal-hydraulic performances could be significantly enhanced by the improved feeding pipe configuration (Design Concept II) for both the two cooling options investigated. Anyway, it has to be underlined that, at this stage of the activity, the design and working conditions of the two cooling options are not mature enough to allow any well-posed comparison of their performances. To this purpose, further solutions are being studied as to both circuit lay-outs and coolant thermodynamic conditions, purposely developed for each cooling option, to allow their future well-posed comparison.

Acknowledgments

This work has been carried out within the framework of the EUROfusion Consortium and has received funding from the Euratom research and training programme 2014–2018 under grant agreement No 633053. The views and opinions expressed herein do not necessarily reflect those of the European Commission.

References

[1] F. Romanelli, et al., Fusion Electricity – A Roadmap to the Realisation of Fusion Energy, European Fusion Development Agreement (EFDA), 2012, 2017 (ISBN 978-3-00-040720-8T).
[2] P.A. Di Maio, et al., Analysis of the steady state hydraulic behaviour of the ITER blanket cooling system, Fusion Eng. Des. 98–99 (2015) 1470–1473.
[3] P.A. Di Maio, et al., Numerical simulation of the transient thermal-hydraulic behaviour of the ITER blanket cooling system under the draining operational procedure, Fusion Eng. Des. 98–99 (2015) 1664–1667.
[4] Final Report on Deliverable DEMO Divertor - Thermo-hydraulic assessmentreport 2015, Report IDM reference No EFDA_D_2MY45W, DIV-1-T001-D010.
[5] J.H. You, G. Mazzone, E. Visca, C. Bachmann, et al., Conceptual design studies for the European DEMO divertor: rationale and first results, Fusion Eng. Des. 109–111 (2016) 1598–1603.
[6] J.H. You, E. Visca, C. Bachmann, T. Barrett, et al., European DEMO divertor target: operational requirements and material-design interface, Nucl. Mater. Energy (2017), http://dx.doi.org/10.1016/j.nme.2016.02.005, in press.
[7] DR-DIV-01-2-Structural feasibility of cassette body material, Report IDM reference No EFDA_D_2N2F23 v1.2.
[8] P.A. Di Maio, M. Merola, R. Mitteau, R. Raffray, E. Vallone, On the hydraulic behaviour of ITER Shield Blocks #14 and #08. Computational analysis and comparison with experimental tests, Fusion Eng. Des. 109–111 (2016) 30–36.
[9] EUROfusion, personal communications.